Journal of Alloys and Compounds 509 (2011) 6595–6598

Contents lists available at ScienceDirect

Journal of Alloys and Compounds

journal homepage: www.elsevier.com/locate/jallcom

Preparations and characterizations of polycrystalline PbSe thin films by a thermal reduction method

D.W. Ma, C. Cheng*

Institute of Laser and Optoelectronic Technology, Zhejiang University of Technology, Hangzhou 310023, PR China

ARTICLE INFO

Article history:
Received 15 July 2010
Received in revised form 16 March 2011
Accepted 17 March 2011
Available online 29 March 2011

Keywords:
Thin films
Semiconductors
Crystal structure
SEM
Optical properties

ABSTRACT

Polycrystalline PbSe thin films were deposited on Si substrates by a thermal reduction method with the carbon as the reducing agent. The X-ray diffraction (XRD) spectra show that the deposited thin films predominately crystallize with the rock-salt structures above the evaporation temperature of 600 °C, and the PbSe thin film has the optimal crystal quality at 900 °C. The scanning electron microscopy (SEM) measurements reveal that the PbSe thin film with carbon addition has uniform crystal grain sizes and dense microstructure, while the thin film without carbon consists of loosely distributed and widely size-ranged crystal grains. The optical transmittance spectrum shows that the direct band gap of the PbSe film is about 0.256 eV. By the introduction of element S, $PbSe_{1-x}S_x$ ($0 \le x \le 1.0$) thin films could be prepared, but excess amount of S additions (>20 at.%) would cause phase segregations between PbSe and PbS phases. The deposition method presented in this paper may be useful for mass-producing polycrystalline lead chalcogenide thin films in the future.

1. Introduction

Thin film semiconductor compounds, especially lead chalcogenide semiconductors and their alloys have caused intensive attention due to their technological importance and future prospects in various electronic and optoelectronic devices [1–3]. PbSe has a narrow direct band gap of 0.28 eV, a positive temperature coefficient of the gap and a large carrier mobility, which makes it widely applicable to fabrication of infra-red detectors, light-emitting devices, solar cells and more recently as infra-red (IR) laser in fiber optics and thermoelectric devices [4–8]. In addition, PbSe is easier to grow, more stable and homogeneous in chemical composition compared with other IR materials like $Cd_{1-x}Hg_xTe$ [5].

So far, PbSe thin films have been prepared by a large variety of techniques such as chemical bath deposition, vacuum deposition, chemical vapor deposition, electro-deposition, molecular beam epitaxy, atomic layer epitaxy, hot-wall epitaxy, pulsed laser deposition, physical vapor transport method and so forth [7,9–16]. In this article, a new and simple thermal reduction method with carbon as reducing reagent was adopted, and polycrystalline PbSe thin films with dense microstructures were deposited on Si substrates. In order to extend the applications of PbSe thin films in IR optoelectronic devices, $PbSe_{1-x}S_x$ thin films were studied preliminarily. In view of the low production cost of this method and the extensive applications of polycrystalline lead chalcogenide thin films in the field of IR optoelectronics, the deposition method is likely to become a practicable way to mass-produce polycrystalline lead chalcogenide thin films in future.

2. Experimental

PbSe and $PbSe_{1-x}S_x$ ($0 \le x \le 1.0$) thin films were deposited on Si substrates by a thermal reduction method. The following chemicals were used as raw materials: chemically pure grade selenium powder (99.95%) and sulphur sublimed (99.5%), analytical grade PbO (99.0%) and activated carbon powder (99.9%). Besides, all the reagents were purchased from Huadong Chemical Reagent Co., Ltd. of China and used without purification. Prior to the deposition experiments, pure Se (S), PbO powders and some carbon powder as the reducing reagent were mixed together in an agate mortar, and Si wafers were rinsed by a standard silicon cleaning method. The deposition process was carried out in a quartz tube furnace with a tube dimension of Φ 35 mm × 1000 mm. As schematically illustrated in Fig. 1, firstly, the furnace was heated to a desired temperature, and then, high purity of N_2 (99.999%) was injected into the quartz tube to eliminate the atmosphere inside. After about 10 min, the mixed raw materials were put in the middle of a quartz boat; then, the quartz boat was rapidly placed into the middle of the horizontal quartz tube furnace, and the cleaned Si wafer was located in a support downstream near the outlet of the furnace body with its surface downward to collect the samples. During the deposition process, the N_2 flow rate was maintained at 5–10 l/min to keep a micro-positive pressure inside the quartz tube, while the other end of the quartz tube was open to the atmosphere. The substrate temperature was varied in the range of 200–450 °C according to different middle furnace body temperatures. After 10 min evaporation, the Si wafer and the quartz tube were drawn out of the furnace and cooled down to the room temperature; the deposited thin film was saved for later tests.

The structures of the synthesized samples were characterized by the XRD measurements, and the morphologies were examined by the field-emission scanning electron microscopy (FE-SEM) measurements, where an energy dispersive X-ray

* Corresponding author. Tel.: +86 571 85290310; fax: +86 571 85290310.
E-mail addresses: dwma@zjut.edu.cn (D.W. Ma), chengch@zjut.edu.cn (C. Cheng).

0925-8388/$ – see front matter © 2011 Elsevier B.V. All rights reserved.
doi:10.1016/j.jallcom.2011.03.100

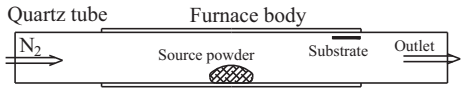

Fig. 1. Schematic illustration of evaporation system for $PbSe_{1-x}S_x$ thin film.

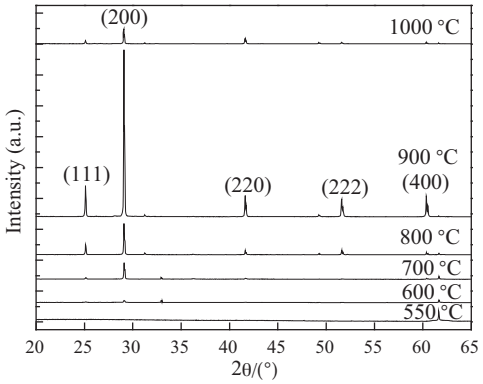

Fig. 2. XRD spectra of PbSe thin films deposited at different temperatures for 10 min.

spectroscopy (EDX) measurement equipped in the FE-SEM instrument was carried out to determine the thin film composition and the presence of impurities. The transmittance spectra of the PbSe thin films were measured, with the Nicolet 6700 Fourier transform infrared (FT-IR) spectrometer.

3. Results and discussion

Fig. 2 shows the XRD spectra of PbSe thin films deposited at different temperatures for 10 min. When the evaporation temperature in the middle of the furnace was around 550 °C, the deposited sample displays only one distinct Bragg diffraction peak beyond the diffraction angle (2θ) of 60°, but from what substance the peak comes is not clear now. However, with the increase of the evaporation temperature up to 600 °C, the peak beyond 60° diffraction angle falls down sharply, and meanwhile the diffraction peaks, the (2 0 0) and (1 1 1) peaks from rock-salt structured PbSe phase come into being. With further increase of the temperature to such degrees as 700 °C or 800 °C, the diffraction peaks from the PbSe phase continue to rise. When the temperature increases to 900 °C, the diffraction peak intensity reaches the maximum, but when the temperature reaches 1000 °C, the diffraction peak intensity declines instead. Therefore, the evaporation temperature of 900 °C can be deemed as the optimal temperature for depositing PbSe thin film. The growth mechanism of the PbSe thin film can be understood from the following chemical reactions: $PbO + C \rightarrow Pb + CO$, $Pb + Se \rightarrow PbSe$. In this experiment, the element carbon serves as the reducing reagent, which favors the formation of Pb clusters, and finally promotes the crystallization and deposition of PbSe thin film. This point will be further clarified in the following control experiments.

Fig. 3 shows the XRD spectra of the PbSe thin films deposited at 900 °C for 10 min. In the two experiments, most raw materials and experimental conditions were the same, except that in one experiment, the carbon was used as the reductant, while in the other, no carbon was used. Obviously, without carbon addition, the deposited sample is still made up of polycrystalline PbSe phase, but the diffraction peak intensity is evidently lowered. This indicates that the sample is of a relatively poor crystal quality. Fig. 4 illustrates the top-view SEM images of the PbSe thin films (a) with and (b) without carbon as the reductant, respectively. Note that with the addition of carbon, the substrate surface is well covered and some cubic-shaped crystalline grains with uniform sizes of 3–5 μm protrude from the surface; the grains are randomly oriented, but they coalesce tightly with their edges interlocked with each other, which indicates a dense microstructure. By contrast, in Fig. 4(b), apparently, the crystalline grains are distributed loosely with some small holes and bumps among the grains, and the grain sizes and morphologies differ considerably. The bigger grains are 3–5 μm in sizes with cubic-shapes, but the smaller ones are only several hundred nanometers with irregular morphologies due to the bad crystallinity. This is consistent with the above XRD results.

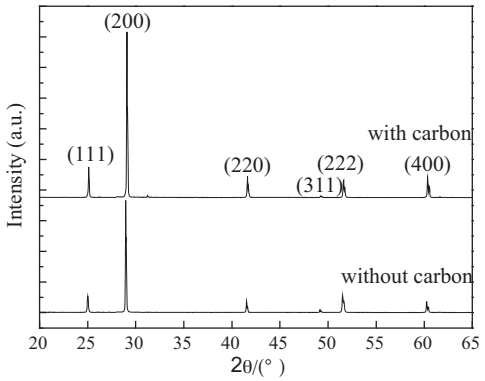

Fig. 3. XRD spectra of PbSe thin films deposited at 900 °C for 10 min with and without carbon as reductant.

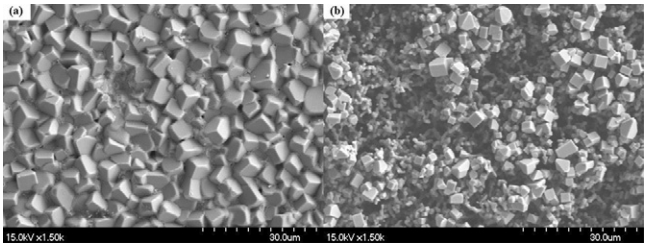

Fig. 4. SEM images of PbSe thin films (a) with carbon and (b) without carbon as reductant.

In order to determine the film composition and evaluate the impurities, the EDX analysis was made. Fig. 5 shows a typical EDX spectrum of PbSe thin film with the reducing reagent of carbon. The approximate atomic ratio of Se to Pb is about 23.0/27.9, slightly deviating from the stoichiometry of the compound PbSe, due to the different evaporation velocities of lead and selenium elements during the preparation process. To prepare PbSe thin film with good stoichiometry, a slightly larger mass ratio of Se to Pb than the ratio used in this experiment may work, while other experimental parameters were kept unchanged. Some impurities of oxygen and carbon were observed also, with the most impurities most likely coming from the air adsorption or contaminations.

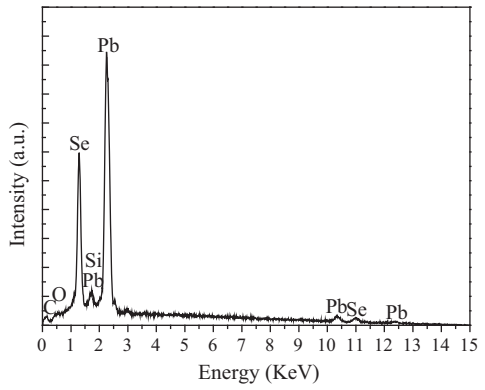

Fig. 5. EDX spectrum of PbSe thin film with carbon as reductant.

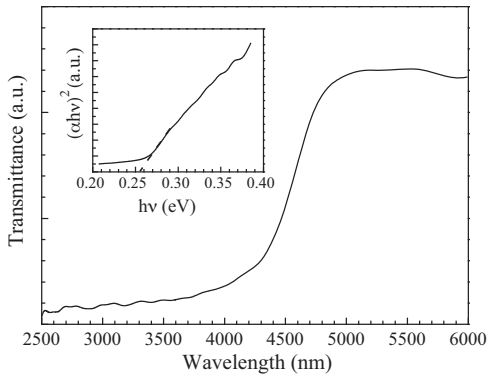

Fig. 6. Transmittance spectrum of PbSe thin film.

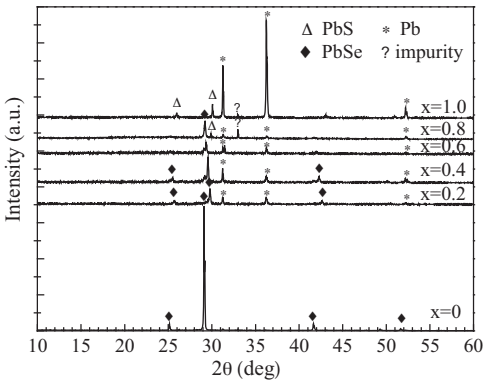

Fig. 7. XRD spectra of $PbSe_{1-x}S_x$ ($0 \le x \le 1.0$) thin films.

As stated above, PbSe is a material of interest in the near infrared region of the electromagnetic spectrum. Therefore, the optical spectra of the PbSe films were taken in the NIR region between 2500 and 6000 nm. Fig. 6 shows a typical transmittance spectrum of PbSe film as a function of incident wavelength. The fall in transmittance at about 4800 nm corresponds to the onset of the fundamental absorption edge indicating the photon energy required to excite an electron across the optical energy band gap of E_g, and the value of E_g can be determined through the following procedures. First, the absorption coefficient α of the film was estimated by the expression: $\alpha = [2.303 \times \log(1/T)]/d$, where T is the transmittance and d the film thickness. Then, the value of α calculated from the relation above was used to plot $(\alpha h\nu)^2$ versus $h\nu$, as shown in the inset of Fig. 6, where $h\nu$ is the photon energy. The linear nature of the plot indicates the existence of the direct transition. By extrapolating the straight line portion to the energy axis at $\alpha h\nu = 0$, the direct band gap E_g of the film is found to be 0.256 eV, smaller than the previously reported value of 0.28 eV for the PbSe bulk material [17]. According to the previous reports [18,19], such factors as the crystal quality and the grain sizes may play important roles in the film band gap. The thermal-evaporated PbSe thin film consists of cubic-shaped crystalline grains, whose crystalline quality is not as good as the perfect PbSe bulk material, and the crystal lattice ions coalesce slightly looser; therefore, the evaluated band gap declines to a smaller value. On the other hand, the band bending is very sensitive to the grain size, and the smaller grain sizes result in the bender band structure, thus leading to a seemingly smaller band gap [19,20]. The adsorption tail in the low energy region seen in the transmittance spectrum is due to considerable contributions from excitonic, free carrier and phonon-assisted direct absorptions and also due to Urbach type absorption in the case of films [21].

In order to extend the applications of PbSe thin films in IR optoelectronic devices, $PbSe_{1-x}S_x$ ($0 \le x \le 1.0$) thin films were prepared at the evaporation temperatures of 850 °C by the introduction of element S. The XRD patterns of the $PbSe_{1-x}S_x$ thin films with different S additions are shown in Fig. 7. It is reasonable that with S addition of 20 at.%, the diffraction peaks from PbSe phase shift towards higher diffraction angles compared with those from pure PbSe thin film, that is $x = 0$, because the lattice constant decreases with S mixing. However, surprisingly in the composition range between 40 and 80 at.%, the diffraction peaks from PbSe shift reversely down to lower diffraction angles. It is assumed that with small amount of S addition, the S will alloy with PbSe completely, that is, homogeneous PbSeS solid solutions will form. But excess introduction of ingredient S will lead to the phase segregations between PbSe and PbS phases. For instance, with S addition of 80 at.%, distinct peaks from PbS phase are observed from the XRD pattern. It is also observed that diffraction peaks from Pb phase emerge with S additions, even with small S addition of 20 at.%. Also for the pure PbS ($x = 1.0$), distinct Pb diffraction peaks appear in the XRD pattern. The reason is that S is more volatile than Se since the boiling points of the simple substances S and Se are 445 and 685 °C, respectively; accordingly, more S evaporates and outflows from the furnace tube, while retaining more Pb in the reaction. As a result, distinct Pb diffraction peaks appear in the samples with $x = 0.2$–1.0, but none from the pure PbSe thin film. Also, note that for the samples with $x = 0.2$–0.8, the Intensities of the diffraction peaks are suppressed severely owing to the multi-phase reactions, and thus more non-crystalline phase comes into being compared with those from pure PbS or PbSe raw materials. It is noticed that for the samples with $x = 0.8$–1.0, one diffraction peak seen in the diffraction angle of about 33° possibly comes from impurity, which is not identified so far.

4. Conclusions

Polycrystalline PbSe thin films were successfully prepared with a novel and simple thermal reduction method. The deposited thin films with the carbon as the reducing agent crystallize with the rock-salt structures and of dense microstructures compared with the loosely distributed microstructures without carbon addition. In order to extend the applications of PbSe thin films in IR optoelectronic devices, $PbSe_{1-x}S_x$ ($0 \le x \le 1.0$) thin films were prepared at the evaporation temperatures of 850 °C. But excess amount of S addition would lead to phase separations between PbSe and PbS; also, Pb phase would separate out from the matrix for the $PbSe_{1-x}S_x$ samples ($x \ge 0.2$). It is believed that the crystalline quality of the $PbSe_{1-x}S_x$ alloy films will be further improved by optimizing the growth parameters such as the evaporation temperature, the ratio of S (Se) to Pb and the increased quantity of carbon etc.

Acknowledgements

This work was supported by the National Natural Science Foundation of China (No. 60777023, No. 60807011) and the Zhejiang Provincial Natural Science Foundation of China (No. Z407371).

References

[1] M. Henini, III–Vs Rev. 7 (1994) 44–49.
[2] H. Zogg, K. Alchalabi, D. Zimin, K. Kellermann, Infrared Phys. Technol. 43 (2002) 251–255.
[3] S. Kumar, B. Lal, P. Aghamkar, M. Husain, J. Alloys Compd. 488 (2009) 334–338.
[4] A. Munoz, J. Melendez, M.C. Torquemada, M.T. Rodrigo, J. Cebrian, et al., Thin Solid Films 317 (1998) 425–428.
[5] A. Mondal, N. Mukherjee, S.K. Bhar, D. Banerjee, Thin Solid Films 515 (2006) 1255–1259.
[6] E. Theocharous, Infrared Phys. Technol. 50 (2007) 63–69.
[7] F. Xiao, C. Hangarter, B. Yoo, Y. Rheem, K.H. Lee, N.V. Myung, Electrochim. Acta 53 (2008) 8103–8117.

[8] V. Sholin, A.J. Breeze, I.E. Anderson, Y. Sahoo, D. Reddy, S.A. Carter, Sol. Energy Mater. Sol. Cells 92 (2008) 1706–1711.
[9] I. Grozdanov, M. Najdoski, S.K. Dey, Mater. Lett. 38 (1999) 28–32.
[10] E.I. Rogacheva, O.N. Nashchekina, Y.O. Vekhov, M.S. Dresselhaus, S.B. Cronin, Thin Solid Films 423 (2003) 115–118.
[11] A. Osherovl, M. Shandalovl, V. Ezersky, Y. Golan, J. Cryst. Growth 304 (2007) 169–178.
[12] Z. Dashevsky, A. Belenchuk, E. Gartstein, O. Shapoval, Thin Solid Films 461 (2004) 256–265.
[13] F. Zhao, X. Lu, J.C. Keay, D. Ray, R. Singh, A. Majumdar, Z. Shi, J. Cryst. Growth 285 (2005) 54–58.
[14] R.S. Mane, C.D. Lokhande, Mater. Chem. Phys. 65 (2000) 1–31.
[15] R.T. Rumianowski, R.S. Dygdala, W. Jung, W. Bala, J. Cryst. Growth 252 (2003) 230–235.
[16] B. Wagner, N.B. Singh, S. McLaughlin, A. Berghmans, D. Kahler, D. Knuteson, J. Cryst. Growth 311 (2009) 1080–1086.
[17] G. Allan, C. Delerue, Phys. Rev. B 70 (2004) 245321–245329.
[18] O. Vigil, F. Cruz, A. Morales-Acevedo, G. Contreras-Puente, L. Vaillant, G. Santana, Mater. Chem. Phys. 68 (2001) 249–252.
[19] D.W. Ma, Z.Z. Ye, J.Y. Huang, L.P. Zhu, B.H. Zhao, J.H. He, Mater. Sci. Eng. B 111 (2004) 9–13.
[20] V. Srikant, D.R. Clarke, J. Appl. Phys. 81 (1997) 6357–6374.
[21] R.P. Vijayalakshmi, R. Venugopal, D.R. Reddy, B.K. Reddy, Semicond. Sci. Technol. 9 (1994) 1062–1068.